行政院國家科學委員會專題研究計畫　期中進度報告

奈米材料的理論研究(1/2)

計畫類別：個別型計畫
計畫編號：NSC91-2113-M-032-005-
執行期間：91 年 08 月 01 日至 92 年 07 月 31 日
執行單位：淡江大學化學系

計畫主持人：王伯昌

計畫參與人員：王鴻偉,廖顯仁,林奕君,葉章弘,陳文豪

報告類型：精簡報告

處理方式：本計畫可公開查詢

中　華　民　國 92 年 5 月 21 日

A Semiempirical Study of Carbon Nanotubes with Finite Tubular Length and Various Tubular Diameters

Bo-Cheng Wang (王伯昌),*[a] Houng-Wei Wang (王鴻偉),[a] I-Chun Lin (林奕君),[a] Yun-Shan Lin (林雲山),[a] Yu-Ma Chou (周　玉)[b] and Houn-Lin Chiu (邱鴻麟) [c]

[a] Department of Chemistry, Tamkang University, Tamsui, Taiwan 251

[b]Department of Physics, Chinese Culture University, Taipei, Taiwan 110

[c] Department of Chemistry, National Kaohsiung Normal University, Kaohsiung, Taiwan 802

Abstract

A semiempirical PM3 quantum computational method has been used to generate the electronic and optimized geometrical structure of SWNT of zigzag and armchair types. We shed light on the electronic structures of SWNT with various diameters and lengths of the tube. Particularly, the calculated HOMO, LUMO and band-gap of SWNT are not monotonic but exhibit a well-defined oscillation, which depends on the tubular diameter and the tubular length. Calculated HOMO, LUMO and band-gap of the zigzag SWNTs have oscillated with tubular diameter as they contain an odd or even number of benzenoids in the circular plane of the carbon nanotube. The zigzag SWNTs with an odd number of benzenoids have a higher band-gap than those of SWNTs with an even number of benzenoids in the circular plane of the carbon nanotube. Calculated results also reveal that the tubular length in the zigzag SWNTs influences the band-gaps very little. For the armchair SWNT, calculated HOMO, LUMO and band-gap contained the oscillate depending on the number of carbon sections in the tubular length axis. Their repeat sections are 3*n*-1, 3*n* and 3*n*+1. The armchair SWNT with 3*n*+1 sections has a high band-gap while the SWNTs with 3*n*-1 sections have a low band-gap. The tubular diameters of armchair SWNT influence the HOMO, LUMO and band gap very little.

*Dedicated to Professor Fa-Ching Chen (陳發淸) on the occasion of his ninetieth

birthday.

Key words: Carbon-nanotube, SWNT, MWNT, AM1.

Running Title: A Semiempirical Study of Carbon Nanotubes

Introduction

Due to the unique physical properties (elasticity, stiffness and deformation) and the applications in various materials (semiconducting, H_2 storage and the probe) of carbon nanotubes, they have attracted considerable attention.[1-5] In 1985 Smalley et al. discovered the truncated-icosahedral C_{60} carbon cluster, named Buckminsterfullerene (also called Buckyball) by laser vaporization of graphite in a high-pressure supersonic nozzle.[6] Almost six years later, Iijima in the NEC research group detected the multi-walled nanotubes (MWNT) in a plasma arc discharge apparatus.[7] In 1993, Iijima and Bethune found the carbon nanotubes made of only one layer (called single walled nanotube, SWNT) by vaporizing graphite and Fe, Co and Ni in an Ar/CH_4 atmosphere.[8, 9] Later, the large-scale purification process and the SEM, TEM and XRD characterization of SWNT were proposed by Rinzler et al.[10] Recently, a number of papers have been published investigating the physical properties, commercial applications and production procedures of SWNT and MWNT.[11-14] The experimental results reveal that the tubular diameters of SWNT can vary ranging from 1.0 *nm* to 1.6 *nm* with a peak maximum at 1.2 *nm*.[10]

According to the geometrical analysis, rolling up a graphene sheet as a hollow cylindrical shapes can form the SWNT. The defect free SMNTs have various types of cylindrical shapes with respect to the array of benzenoids in the carbon nanotube. According to the structure of the array of benzenoids, there exist armchair tubules,

zigzag tubules and chiral tubules among SWNTs. Ebbesen used the hexagonal network of a single graphite sheet to give a simple description of the geometrical relation in SWNT.[15] Theoretically, the SWNT with the armchair type roll up of the graphite sheet in the [2,1,0] direction which could be defined as a σ_v symmetry element in a benzenoid ring (Fig. 1), also generated the SWNT with zigzag tubules being in a [1,0,0] rolling direction, which is a σ_d symmetry element in a benzenoid ring (Fig. 1). These two rolling up directions differ by 30^o, 60^o and 90^o. Theoretically, Saito and Hamada investigated their physical properties and found that they can be from metallic to semi-conducting, based on the tubular diameter and chirality.[16]

Recently, Erkoç et al. used the empirical many-body potential energy function to investigate the energies of carbon nanotubes.[17] Then, Rochefort et al. have studied the electronic structure of finite-length SWNT of the armchair type using semiempirical and *ab initio* computational methods.[18] Türker et al. used the semiempirical AM1 method to investigate the molecular orbital properties of SWNT of the zigzag type.[19] They predicted that the physical properties of SWNT should strongly depend on tubular diameter. Yoshizawa *et al.* used the semiempirical CNDO/2 method to compute band-gap oscillations in polyphenanthrenes, which represent a segment of SWNT, depending on their molecular orbitals.[20] Also, Bernhole used *ab initio* molecular dynamic calculation to simulate the growth of nanotubes.[21] Very recently, Li et al. used DFT and semiempirical PM3 to simulate armchair carbon nanotubes and compared them with STM experiments.[22, 23]

To pursue the effect of tubular length and tubular diameter in SWNT, a small segment of SWNT of different types has been used for calculations in this study. The semiempirical PM3 method was used to determine the geometry-optimized, electronic structures and molecular energies of SWNTs of the zigzag and armchair types with different tubular diameters and tubular lengths. Calculated HOMO, LUMO and

band-gap (the energy difference between HOMO and LUMO) of SWNTs allow us to predict some physical properties of SWNT. For understanding the segment of SWNTs in more detail, the molecular orbital and electronic structures of polycyclic benzenoids have been calculated by using *ab initio* DFT/B3LYP with a 6-31G basis set.

Computations

According to the geometrical analysis, a SWNT is either being achiral (zigzag, armchair) or achiral (helicity) (Fig. 1) in structure. In this work, we selected the zigzag and the armchair SWNTs for calculations. The SWNTs are defined as open-ended and defect free. To evaluate physical properties of SWNTs in the quantum mechanical calculation, hydrogen atoms substituted the dangling bonds on both ends.

The semiempirical PM3 computational method that was used in this work is implemented in the MOPAC program package.[24] All the calculations were performed in the RHF framework for closed shell species. In order to confirm the electron transition properties in the circumference of SWNT, the related polyacene and polycyclic benzenoid segments were calculated by using the DFT/B3LYP method with the 6-31G basis set. The DFT calculations were performed employing the Gaussian 98 package.[25]

The geometric structure of SWNT could be described in terms of a role up vector (n, m), which denotes the unit vectors of the hexagonal honeycomb lattice, and n and m are integers, describing the tubular diameter (or the chiral vector) and the tubular length (or the translational vector), respectively. For the zigzag type SWNT (Fig. 1), n and m denote the number of benzenoids in the circumference of the tube (the chiral vector) and the number of trans-polyene rings along the axis of the tubular length (the translational vector), respectively. Alternatively, the armchair type SWNT (Fig. 1), n

and m denote the number of benzenoids in the circumference of the tube (the chiral vector) and the number of sections in a single circumference along the tubular length axis (the translational vector). Since the chiral nanotubes were not considered, Saito's formula for describing carbon nanotubes was not used in this study.[14]

Results and Discussion

A. Geometrical considerations

Fig. 1 shows the hexagonal network of a single graphite sheet. Particularly, the zigzag type SWNT is obtained by rolling up hexagons with the σ_d reflection plane. The carbon atoms of the zigzag type SWNT arrange as cis-polyenes with a single circular plane of carbon atoms. On the other hand, the armchair type SWNT is obtained by rolling up hexagons as the σ_v symmetry plane so that the carbon atoms arrange as trans-polyenes with a single circular plane of carbon atoms.

In order to evaluate the influence of the tubular length and the tubular diameter on the electronic properties of the SWNT, the following simple mathematic formulas relating the tubular diameter of SWNT with the number of benzenoids in the circular plane of the carbon tube were used: For the zigzag SWNT, $X = [r\cos(\pi/6)]/[\sin(\theta/2)]$, where $\theta = \pi/n$, $2X$ is the tubular diameter, r is the length of C-C bond in the carbon nanotube which was set to be 1.42 , and n is the number of benzenoids in a single circular plane of SWNT. For instance, the average tubular diameter of SWNT is 1.2 *nm,* so it may contain 14 benzenoids in a single circular plane according to this formula. For the armchair SWNT, $X = r/(\sin\theta)$, $\theta = 2\pi/3n$ and $2n$ is the number of benzenoids in a single circular plane of SWNT. Experimentally, the tubular diameter of a regular SWNT is 1.2nm, which may contain 16-18 benzenoid rings in a single circular plane of armchair SWNT. These mathematical formulas can be extended to larger scale carbon-nanotube systems.

B. Quantum mechanical consideration

To investigate the influence of the tubular length and tubular diameter of SWNTs, various geometric optimized structures and electronic structures of SWNT with zigzag and armchair types were calculated by the semiempirical PM3 method. We performed electronic structure calculations for (*n*, 6) to (*n*, 10) in the various tubular diameters and (6, *m*) to (14, *m*) in the tubular length for both zigzag and armchair SWNTs, respectively. According to these calculations, (14, *m*) SWNT is very close to the experimental carbon nanotube. Because of the computer limitations, we performed the calculation of the tubes with tubular lengths under 10 nm.

Zigzag type SWNT

Figs. 2a and 2b show the band-gaps of zigzag SWNT calculated by the semiempirical PM3 method with different tubular diameters and tubular lengths. In Fig. 2a, we illustrated the influence of the tubular diameter on the properties of zigzag SWNTs. Calculated band-gaps of zigzag SWNT exhibit oscillations with *n* being an odd or even integer. Particularly, *n* is the number of benzenoids in the circumference of the tube so that it contains 2*n* carbon atoms in a single circular plane. We observed that the band-gap of the tube with even *n* is lower than that of tubes with odd *n*. The difference in the energy band-gaps for the (6, 2) and (7, 2), (7, 2) and (8, 2) tubes are 0.67 eV and –0.84 eV, respectively. Similarly, the HOMO and LUMO of zigzag SWNT also show oscillations. For the SWNT with infinite tubular length, we assume that the oscillation amplitude decreases and the band-gap value slowly converges to zero. In order to confirm the oscillation properties of zigzag SWNTs, we used the DFT/B3LYP method with the 6-31G basis set to calculate polycyclic benzenoids with acene-edge type (which is a small segment of the zigzag SWNT) containing 6, 7, 8

and 9 benzenoids along the circumference (denoted as polycyclic benzenoid(n) with n benzenoids) (Figs. 3a and 3b). According to Fig. 3b, the calculated HOMO molecular orbital for the polycyclic benzenoid(6), which contains six benzenoid rings, has an anti-bonding character along the circumference of the tube, while the LUMO also has the antibonding character. We predict that the energy difference between HOMO and LUMO is small. Meanwhile, the HOMO and LUMO for polycyclic benzenoid(8) shows the same trend as that for polycyclic benzenoid(6) and has a low band-gap. The HOMO of polycyclic benzenoid(7) has a bonding character along the circumference of the tube, and the LUMO has an anti-bonding character. Thus, the HOMO orbital energy decreases and LUMO energy increases, which leads to a high band-gap between HOMO and LUMO. We can conclude from the molecular orbital analysis that polycyclic benzenoids with an odd number of benzenoids have higher band-gaps than those with an even number of benzenoids. The molecular diagram showed that polycyclic benzenoids do not have a bonding character, and the interaction between two cis-polyene sections is very small. Thus, a single cis-polyene chain may play a very important role for the electron transition in the zigzag SWNTs. In particular, this calculation results for polycyclic benzenoid show the same trend as those for zigzag SWNTs with different tubular diameters. We conclude that the polycyclic benzenoid could be the building fragment during the growth of the carbon nanotube.

The calculated HOMO, LUMO and band-gap of zigzag SWNT with different tubular lengths and finite tubular diameters are presented in Fig. 2b. One can see that the tubular length of zigzag SWNT does not affect the oscillation amplitude for HOMO, LUMO and band-gap. We thus shed light on the electronic structure of zigzag type SWNT with a cis-polyene chain. Recently Rochefort's group found similar influence of the nanotube diameter on the band-gap for the [6, 6] to [10, 10] zigzag SWNT, which have close values for HOMO, LUMO and the band-gap and

exhibit the same oscillatory behavior. Our calculation results therefore confirmed Rochefort's calculation result.[18]

Armchair type SWNT

Recently, several papers have been published considering the electronic structures of armchair SWNT by using computational methods.[17-19] They predicted that the HOMO/LUMO and band-gap of the SWNTs with the armchair type have oscillation properties with the repeat unit having $3n$-1, $3n$ and $3n$+1 models (n is integer) in the carbon section along their latitudes. Yoshizawa also used polyphenanthrenes and finite graphite sheet to describe these properties.[19] In this paper, we used the semiempirical PM3 method to calculate the HOMO, LUMO and band-gap of armchair SWNTs with different tubular diameters and tubular lengths and used the DFT/B3LYP/6-31G to compute the electronic structure of related polycyclic benzenoids of the armchair type. The band-gaps of armchair SWNT with various tubular lengths and tubular diameters are shown in Figs. 4a and 4b. Because of the computing capacity limitations, we calculated [8, m], [10, m], [12, m] and [14, m] armchair SWNTs and compared the energies for tubular lengths. One can see that the band-gaps for armchair SWNT have an oscillatory behavior with $3n$-1, $3n$ and $3n$+1 repeating unit in the carbon section. Particularly, the highest band-gap was obtained for the $3n$ + 1 section and the $3n$ + 2 section has a small amplitude. For instance, we found the band-gap of 6.72eV, 5.42eV, 4.99eV and 5.51eV for [12, 4], [12, 5], [12, 6] and [12, 7] armchair SWNTs, respectively. The [12, 4] tube has the highest value, while [12, 6] has the lowest one. The energy band-gaps of armchair SWNT with the same tubular length and various tubular diameters are presented in Fig. 4b. For the armchair SWNT, the band-gap increases approximately by 0.1 – 0.2 eV, while the tubular diameter increases by two benzenoids. We conclude that the band-gap of

armchair SWNT changes very little depending on the tubular diameter. Thus, the tubular diameters of armchair SWNT do not influence the oscillation amplitude of HOMO/LUMO and band-gaps. Alternatively, the cis-polyene located along the circumference of armchair SWNT, may not play a significant role in the electron transition in the tube.

In order to confirm this band-gap oscillation behavior for armchair SWNT, we used the DFT/B3LYP calculation with the 6-31G basis set to determine the electronic structure of the (8, 3) to (8, 6) and (10, 4) to (10, 6) polycyclic benzenoids (armchair type). The band-gaps and molecular orbitals of these polycyclic benzenoid (armchair type) are shown in Figs. 5a and 5b. According to Fig 5a, the DFT calculated band-gaps of the (8, *m*) series of polycyclic benzenoids exhibit the same trend as that for armchair SWNTs. The band-gap for (8, 4) is higher than that of (8, 5) and (8, 6). The molecular orbital analysis for (8, 4) (Fig. 5b) shows that its HOMO has a bonding character and LUMO has an anti-bonding character along the tubular length axis. This may lead to a high band-gap. Similarly, both HOMO and LUMO have a bonding character so that it generates a low band-gap for (8, 6) polycyclic benzenoids.

Conclusion

In the present work, *ab initio* and semiempirical calculations were used to investigate the geometrical and electronic structures of zigzag and armchair types SWNT. The semiempirical PM3 calculations reveal that the HOMO, LUMO and energy band-gaps of zigzag SWNT have an oscillatory behavior depending on the number of benzenoids along the peripheral circuit of the tube and the tubular length does not affect the oscillation amplitudes. In contrast, the tubular length of armchair SWNTs influences the oscillation amplitudes of HOMO, LUMO and band-gap depending on the carbon sections along the tubular length axis. The tubular diameter

of armchair SWNT influenced the HOMO, LUMO and band-gap slightly. This calculation provides important information on the properties of SWNT needed for the design of new nano-electronic devices.

Acknowledgment

We thank Dr. Alexander Mebel for reading the manuscript and the National Science Council of ROC for support.

References

1. Ajayan, P. M.; Stephan, O.;. Colliex, C;. Trauth, D. *Science*, **1994**,*265*, 1212.
2. Saito, Y.;. Hamaguchi, K.; Hata, K.; Uchida, K.; Tasaka, Y.; Ikazaki, F.; Yumura, M.; Kasuya, A.; Nishina, Y. *Nature*, **1997,** 389, 554.
3. de Heer, W. A.; Chatelain, A.; Ugarte, D. *Science*, **1995**, 270, 1179.
4. Collins, P. G.; Zettl, A.; Bando, H.; Thess, A.; Smalley, R. E. *Scienc*e**, 1997**, 278, 100.
5. Nardelli, M. B.; Yokobson, B. I.; Bernholc, J. *Phys. Rev. B*, **1998**, 57, R4277.
6. Kroto, H. W.; Heath, J. R.; O'Brien, S. C.; Curl, R. F.; Smalley, R. F. *Nature***, 1985**,18, 162.
7. Iijima, S. *Nature***, 1991**,354, 56.
8. Iijima, S.; Ichihashi, T. *Nature***, 1993**,63, 603.
9. Bethune, D. S.; Kiang, C. H.; de Vries, M. S.; Gorman, G..; Savoy, R.; Vazquez. J.; Beyers, R. *Nature*, **1993**, 363, 605.
10. Rinzler, A.G.; Liu,J.; Dai,H.; Nikolaev, P.; Huffman, C.B.; Rodriguez-Macias, F. J.; Boul, P. J.; Lu, A. H.; Heymann, D.; Colbert, D. T.; Lee, R. S.; Fischer, J. E.; Rao, A. M.; Eklund, P. C.; Smalley, R. E. *Applied Physics A***, 1998**,67, 29.

11. de Heer, W. A.;Chatelain, A; Ugarte, D. *Science*,**1995**,270, 1179.
12. Rinzler, A. G.; Hafner, J. H.; Nikolaev, P.; Lou, L.; Kim, S. G.; Tomanek, D.; Nordlander, P.; Colbert, D. T.; Smalley, R. E. *Science*, **1995**,269, 1550.
13. Kong, J.; Franklin, N. R.; Zhou, C. W.; Chapline, M.; Peng, G. S.; Cho, K. J.; Dai, H. J. *Science*, **2000**,287, 622.
14. Saito, R.; Dresselhaus, G..; Dresselhaus, M. S. *Physical Properties of Carbon Nanotubes*, *Imperial College Press*, **1998**, London.
15. Ebbesen, T. W. *Acc. Chem. Res.*, 1998. 31, 558.
16. a. Saito, R.; Fujita, M.; Dresselhaus, G..; Dresselhaus, M.S. *Phy Rev.*,**1992**, *B46*, 1894. b. Hamada, N.; Sawada, S.; Oshiyama, *A. Phys. Rev. Lett.*, **1993**, 68, 1579.
17. Erkoç, ª .; Özkaymak, S. *Eur. Phys. J.*, **1998,** *D 4*, 331.
18. Rochefort, A.; Salahub, D. R.; Avouris, P. *J. Phys. Chem. B*, **1999**, 103, 641.
19. Türker, L.; Erkoç, ª . *J. Mole. Stru. (Theochem)*, **2002**, 577, 131.
20. Yoshizawa, K.; Yahara, K.; Tanaka, K.; Yamabe, T. *J. Phys. Chem. B*, **1998**,102, 498.
21. Bernhole, J.; Brabec, C.; Nardelli, M. B.; Maiti, A.; Roland, C.;. Yakobson, B. I. *Appl. Phys.,* **1998**, *A 67*, 39.
22. Li, J.; Zhang, Y.; Zhang, M. *Chem. Phys. Lett.,* **2002**,364, 328.
23. Li, J.; Zhang, Y.; Zhang, M. *Chem. Phys. Lett.,* **2002**,364, 338.
24. Stewart, J. J. P. Fujutsu Limited, Tokyo, Japan **1993**.
25. Frisch, M. J.; Trucks, G. W.; Schlegel, H. B.; Scuseria, G. E.; Robb,; Cheeseman, J.R.; Zakrzewski, V. G.; Montgomery, J. A.; Stratmann, R. E.; Burant, J. C.; Dapprich, S.; Millam, J. M.; Daniels, A. D.; Kudin, K. N.; Strain, M.C.; Farkas, O.; Tomasi, J.; Barone, V.; Cossi, M.; Cammi, R.; Mennucci, B.; Pomelli, C.; Adamo, C.; Clifford, S.; Ochterski, J.; Petersson, G. A.; Ayala, P. Y.; Cui, Q.; Morokuma, K.;. Malick, D. K; Rabuck, A. D.; Raghavachari, K.; Foresman, J. B.;

Cioslowski, J.; Ortiz, J. V.; Stefanov, B. B.; Liu, G..; Liashenko, A.; Piskorz, P.; Komaromi, I.; Gomperts, R.; Martin, R. L.; Fox, D. J.; Keith, T.; Al-Laham, M. A.; Peng, C. Y.; Nanayakkara, A.; Gonzalez, C.; Challacombe, M.; Gill, P. M. W.; Johnson, B. G.; Chen, W.; Wong, M. W.; Andres, J. L.; Head-Gordon, M.; Replogle, E. S.; Pople, J. A.; Gaussian 98, Gaussian, Inc., Pittsburgh, **1998.**

Figure captions

Fig. 1 Hexagonal network of a single graphite sheet for zigzag, armchair and chiral SWNT

Fig. 2a Semiempirical PM3 calculated band-gaps for zigzag SWNT with various

tubular diameters.

Fig. 2b Semiempirical PM3 calculated band-gaps for zigzag SWNT with various tubular lengths.

Fig. 3a DFT calculated band-gaps for polycyclic benzenoids (zigzag type).

Fig. 3b DFT calculated molecular orbitals for polycyclic benzenoids (zigzag type).

Fig. 4a Semiempirical PM3 calculated band-gaps for armchair SWNT with various tubular diameters.

Fig. 4b Semiempirical PM3 calculated band-gaps for armchair SWNT with various tubular lengths.

Fig. 5a DFT calculated band-gaps for polycyclic benzenoids in the (8, 3) to (8, 6) and (10, 4) to (10, 6) (armchair type) series.

Fig. 5b DFT calculated molecular orbitals for polycyclic benzenoids in the (8, 3) to (8, 6) (armchair type) series.

Fig. 1

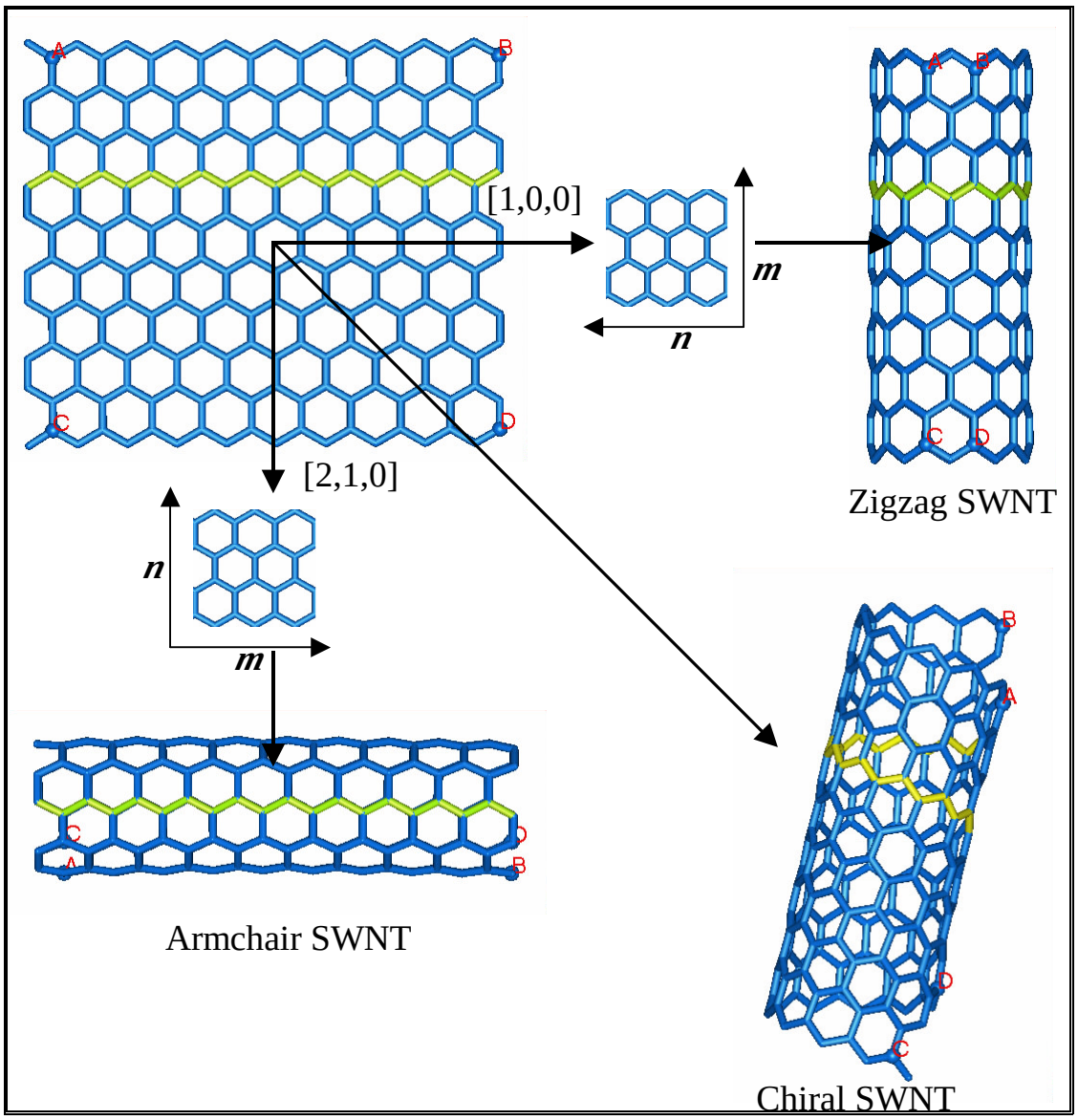
A
B
C
D
[1,0,0]
m
n
[2,1,0]
n
m
Zigzag SWNT
Armchair SWNT
Chiral SWNT

Fig. 2a

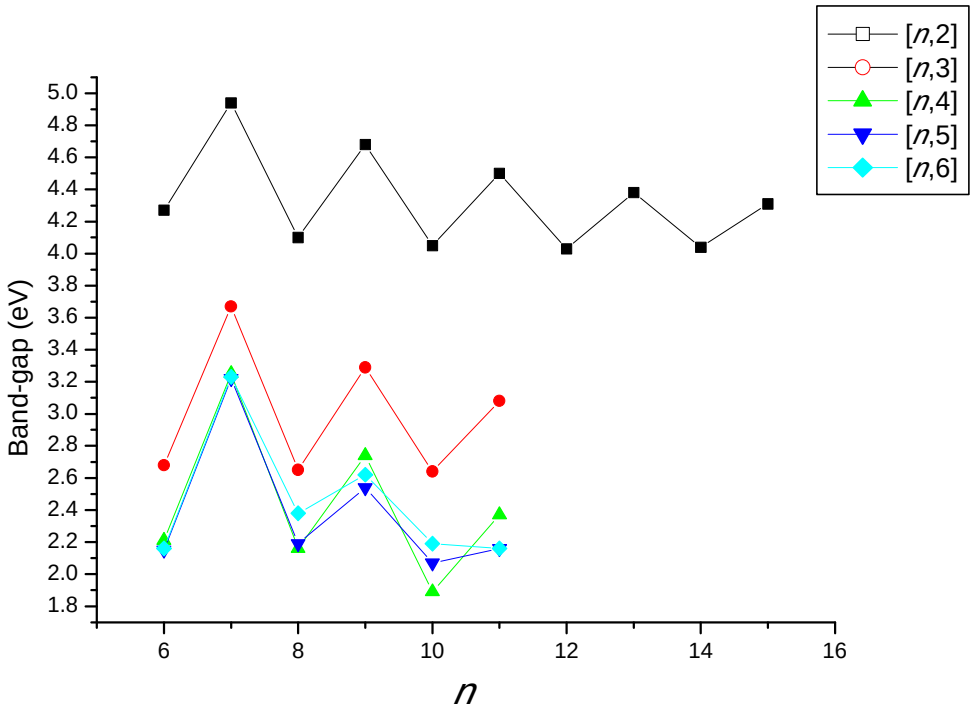
[n,2]
[n,3]
[n,4]
[n,5]
[n,6]
Band-gap (eV)
5.0
4.8
4.6
4.4
4.2
4.0
3.8
3.6
3.4
3.2
3.0
2.8
2.6
2.4
2.2
2.0
1.8
6
8
10
12
14
16
n

Fig. 2b

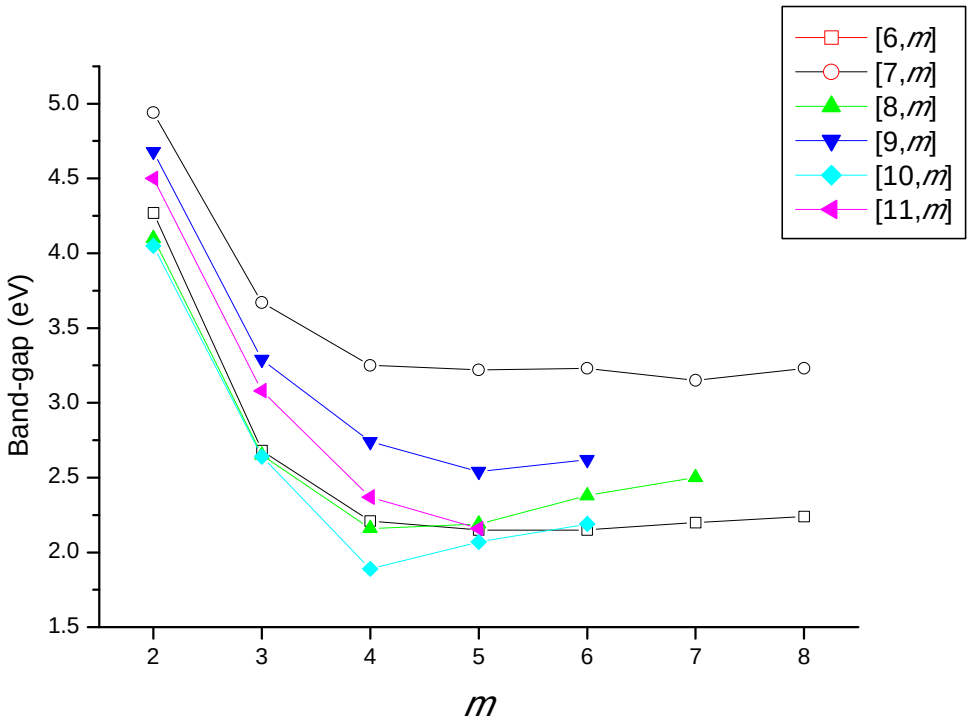

Fig. 3a

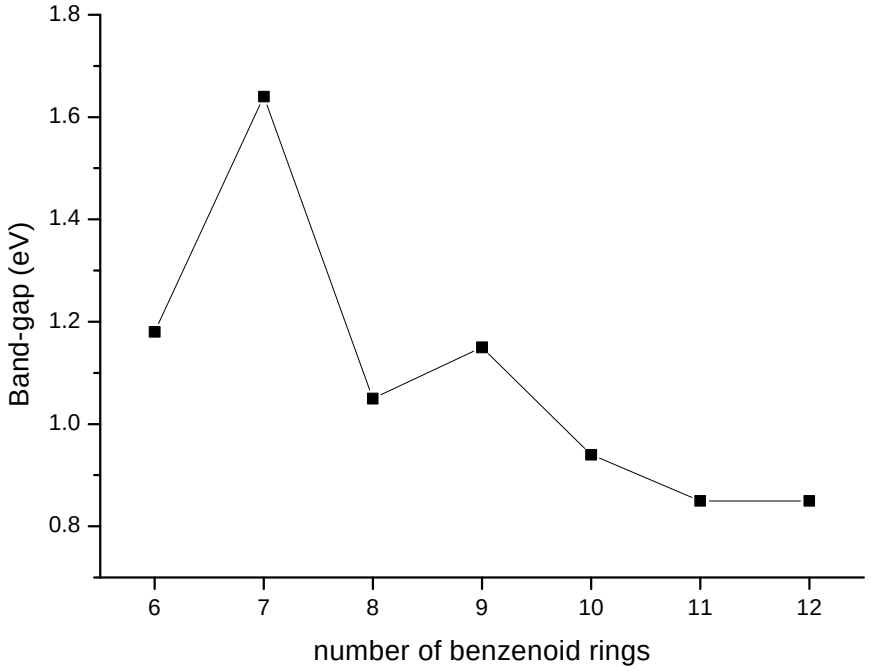
Band-gap (eV)
1.8
1.6
1.4
1.2
1.0
0.8
6
7
8
9
10
11
12
number of benzenoid rings

Fig. 3b

	HOMO	LUMO
(6,2)	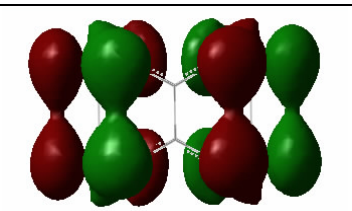	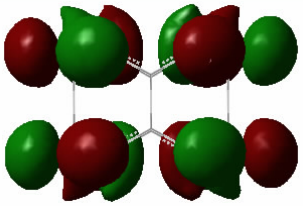
(7,2)	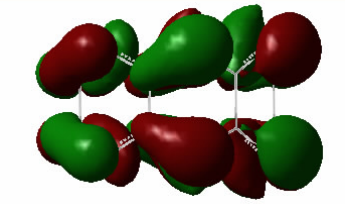	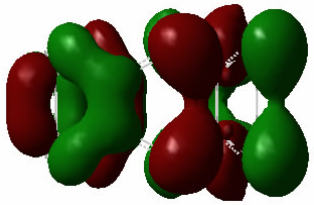
(8,2)	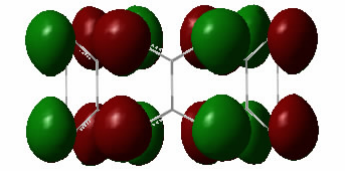	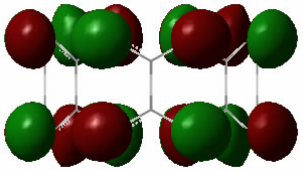
(9,2)	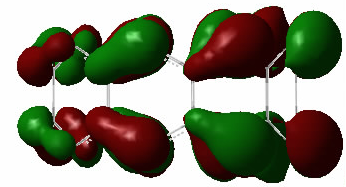	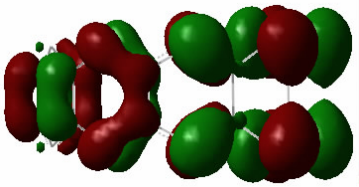
(10,2)	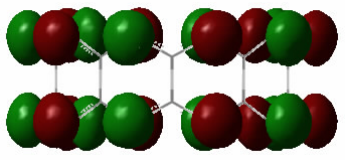	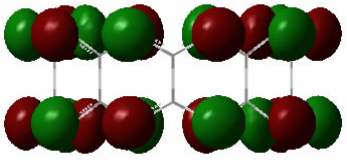
(11,2)	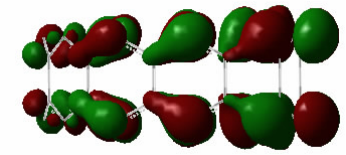	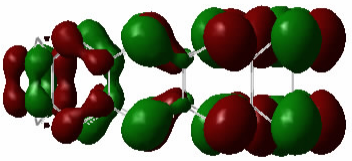
(12,2)	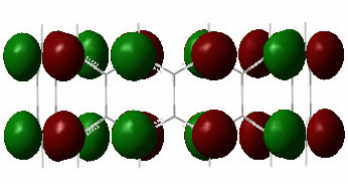	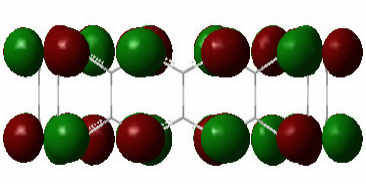

Fig. 4a

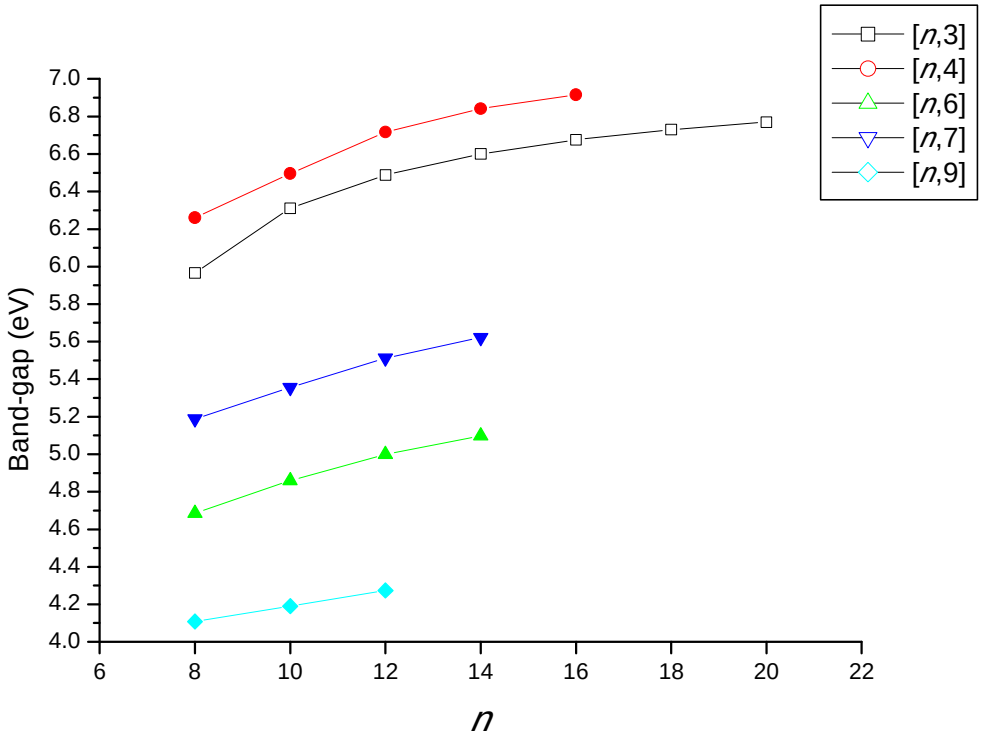
[n,3]
[n,4]
[n,6]
[n,7]
[n,9]
Band-gap (eV)
7.0
6.8
6.6
6.4
6.2
6.0
5.8
5.6
5.4
5.2
5.0
4.8
4.6
4.4
4.2
4.0
6
8
10
12
14
16
18
20
22
n

Fig. 4b

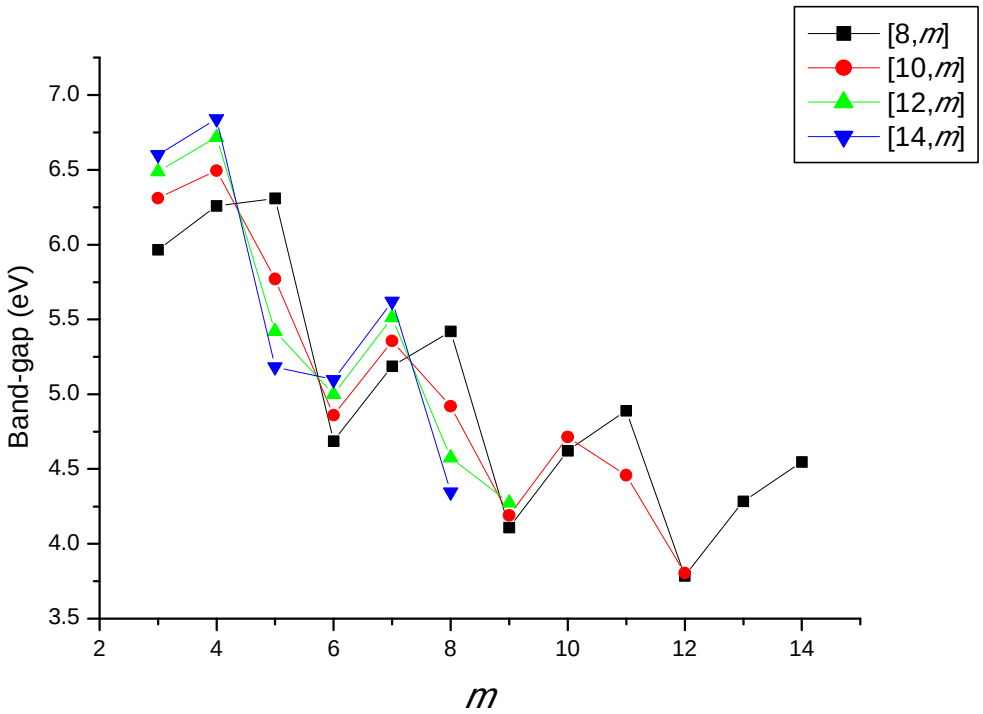

Fig. 5a

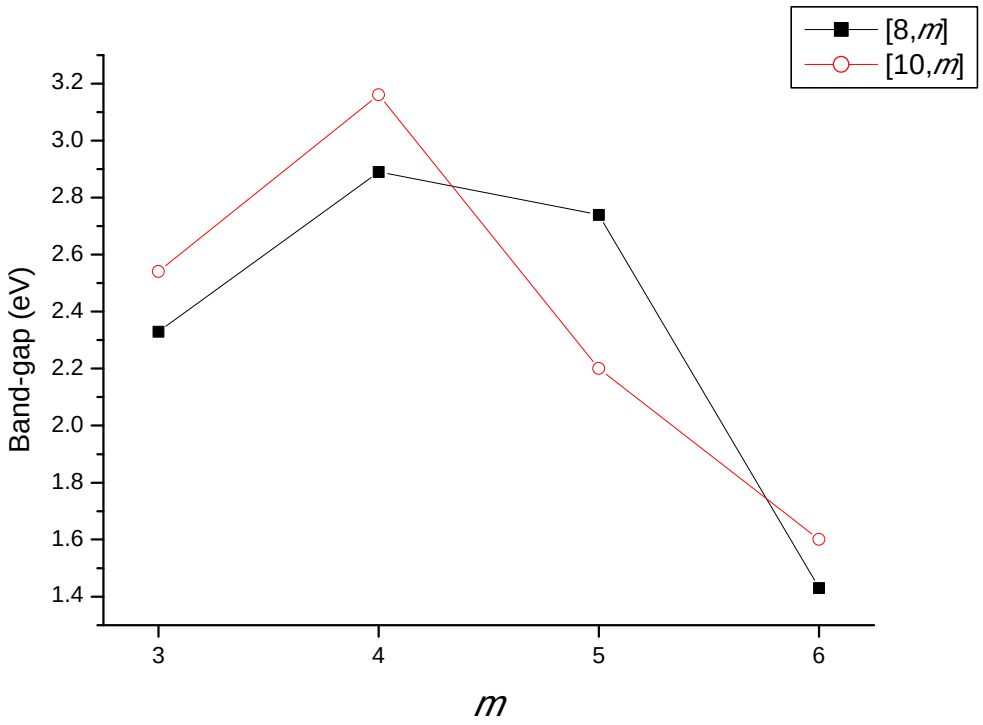

Fig. 5b

	HOMO	LUMO
(8,3)	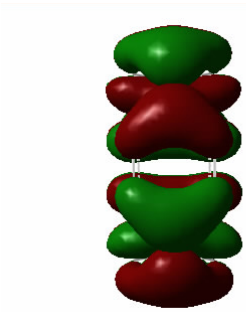	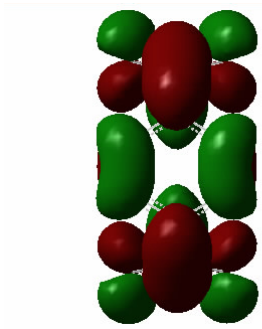
(8,4)	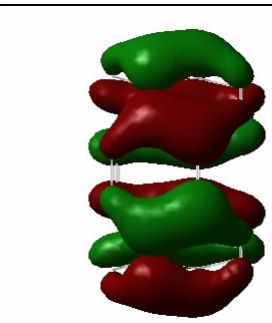	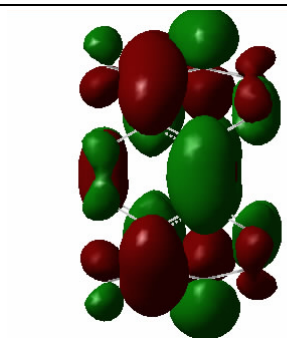
(8,5)	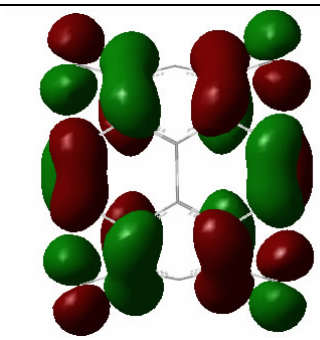	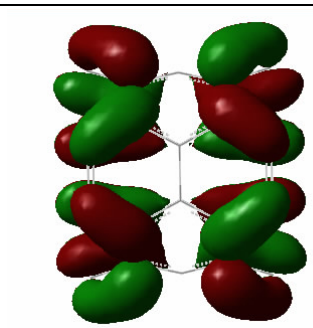
(8,6)	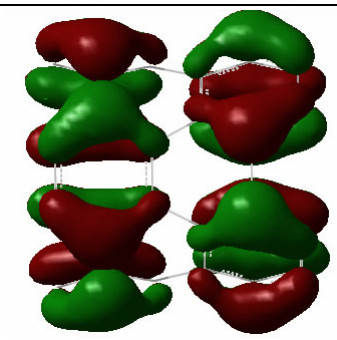	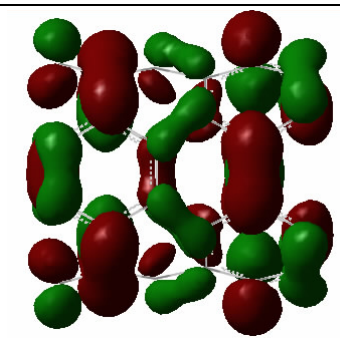

Bo-Cheng Wang,[*a] Jiang-Chiang Chang,[a] Jiunn-Hung Pan[a], Cuihua Xue[b] and Fen-Tair Luo[b]

[a]Department of Chemistry, Tamkang University, Tamsui, Taiwan 251

[b]Institute of Chemistry, Academia Sinica, Taipei, Taiwan 115

Abstract

Recently, the distyrylbenzene (DSB) derivatives have been synthesized and used as a dopant in the multiplayer OLED fabrication. Computational methods (the semiempirical AM1 for optimized geometries and ZINDO for excitation energy) have been used to calculate the absorption and emission spectra of a series of DSB derivatives. These derivatives may contain electron-withdrawing and electron-donating substituents. These substituents have been studied at various positions in a DSB moiety to compute their photo-physical properties and electroluminescent behavior in OLED. The HOMO, LUMO, ΔE (between HOMO and LUMO), excitation energy, absorption λ_{max}, oscillator strength and emission λ_{max} in these derivatives have been also calculated in this paper. Presumably, the procedures of theoretical calculation can be employed to predict the electro-luminescence characteristics of other materials, and further, to design novel materials for OLED.

Introduction

During the last decade, the research in the organic electroluminescent (EL) materials has become one of the most interesting topics in fields of chemistry, physics and materials science.[1-6] In 1970, Hörhold *et al.* reported the optical, electronic and

photoelectronic properties of poly-*para*-phenylene vinylene (PPV).[7] Seventeen years later, Tang and VanSlyke in Kodak fabricated an organic EL device using organic thin film.[8] Recently, PPV derivatives have found wide applications in EL devices.[9, 10] A series of DSB derivatives, which are the repeating unit of PPV, have been developed and applied as a light-emitting diode in emissive materials.[11] Recently, Luo *et al.* generated DSB derivatives, which contain an electron-withdrawing cyano group and various alkyl or alkoxy groups on the vinylene and phenylene moieties and can be applied as an emitter in organic light emitting diode (OLED).[12] In particular, the substituents in the DSB derivatives could improve the photoluminescent quantum yield or tune the emission wavelength. According to the experimental results, the blue emission was achieved with these DSB derivatives as dopant, in a device of structure ITO/NPB/CBP/TPBI : DSB/TPBI/Mg : Ag.[12] Recently, Ichino *et al.* observed the optical spectra of DSB derivatives with methoxy substituents at the central and/or the terminal phenyl subunits.[13]

PPV materials have been extensively studied theoretically by using different calculation methods to generate their electronic and geometric structures, HOMO, LUMO, absorption and emission spectra.[14-16] Yu *et al.* determined the ground and excited states of DSB using *ab initio* method at the SCF level with 6-31G basis set and INDO/S-CIS method, respectively.[15]

In this work, the semiempirical and *ab initio* calculation methods are used for generating the geometrical and electronic structures, electronic transition energies (absorption and emission) and intensities (oscillator strengths) for DSB and its derivatives. Then, the calculated energies are calibrated based on a comparison with the experimental data for a series of DSB derivatives. The effects of substituent and their positions from electron-donating and electron-withdrawing groups on DSB derivatives are also investigated. In particular, the substitution position can be in the

central and terminal phyenylene as well as vinylene subunits of a DSB molecule. These calculations can be used as a model system for understanding the relationship between luminescence and molecular structure and also used in fabricating multi-layer-type EL devices.

Computations

Distyrylbenzene (DSB) and its derivatives are oligomers of PPVs with short chain lengths. The geometries of DSB and its derivatives have been fully optimized at the semiempirical AM1 and PM3 as well as *ab initio* at the RHF/6-31G and DFT/B3LYP/6-31G levels (Table 1). Then, the semiempirical AM1 method was used to optimize the ground state structure of DSB derivatives with various substituents in different substitution positions. Electronic transition energies (absorption and emission) and intensities (oscillator strengths) of DSB derivatives were obtained using the semiempirical ZINDO (INDO/3) method and will be referred to as the "ZINDO/method", where "method" is the level of geometry optimization. In general, the ZINDO method has been parameterized to reproduce excitation energies and should be very useful. The semiempirical AM1, PM3 and ZINDO methods are implemented in MOPAC97 and *ab initio* (HF and DFT) methods are implemented in Gaussian 98 program packages.[18, 19] The excitation energy calculations in this paper were limited to the first excited electronic state corresponding to the HOMO – LUMO single excitation.

Result and Discussion

According to the geometrical analysis, there exist two isomers of DSB, including trans, cis- and trans, trans- DSB (compound 1). Yu *et al.* calculated the absorption and emission spectra of these DSB isomers using *ab initio* methods and found in accord with their experiments.[15] Electronic spectra involving transition of valence electrons

occurs in the UV/VIS region and they were studied theoretically both absorption and emission. In order to investigate the effect of various substituents, the substitutions were introduced at the central phenylene, the vinylene and the terminal phenylene subunits in a DSB moiety. A series of DSB derivatives (Fig. 1) were investigated by the semiempirical AM1 method for the optimized structure and ZINDO for the excitation energies.

Table 2 shows the calculated HOMO/LUMO energy, ΔE (= LUMO - HOMO), the absorption λ_{max}, the oscillator strength and the emission λ_{max} for these mono-substituted DSB derivatives with substitution at the central phenylene subunit. In particular, the differences of the calculated excitation energies (3.43 eV, 3.42 eV, 3.42 eV and 3.42 eV) and absorption λ_{max} (362 *nm* corresponds to 390 *nm* in experiment) of methoxy, ethoxy, propoxy and hexyloxy substituents (Compounds 2-5) in the central phenylene subunit are very small. The calculated emission (fluorescence) λ_{max} for these DSB derivatives is about 388 *nm*. These calculated excitation energies decrease by about 0.16 eV as compared to the DSB without substituents. Therefore, the DSB derivatives with alkyloxy substituents in the central phenylene exhibit a red shift relative to the DSB without any substituent. The decrease of the excitation energy (or energy band gap) in these derivatives leads to a decrease of oxidation potentials (increase of the HOMO orbital energy). In order to facilitate the calculation efficiency, the methoxy group was used to replace hexyloxy group in the further study of DSB derivatives.

Compounds 6 and 7 are α- and β-substituted DSB where the substituent is positioned in the vinylene near the central phenylene and the terminal phenylene, respectively. In particular, when the α- cyano group is adjacent to the central phenylene, a steric interaction will be generated with the alkoxy group, which is located in the central phenylene of a DSB moiety. According to the semiempirical

AM1 calculation, this distortion increase the dihedral angle between the central phenylene and the vinylene subunit by about 50 °. Theoretically, this distortion in the main chain of DSB may reduce the degree of π-conjugation. Since the β-cyano group does not interact with the alkoxy group on the central phenylene, the calculated excitation energy for compound 6 is 0.19 eV higher than that for compound 7 (3.36 eV *vs.* 3.17 eV). This energy difference generated a blue shift of 22 *nm*. According to the above calculation results, we conclude that a shorter conjugation length will cause larger LUMO – HOMO band gap (or excitation energy) and cause the blue shift in DSB derivatives.

In order to investigate the influences of substituents in the terminal phenylene subunit of DSB, we calculated the derivatives with the *ortho-*, *meta-* and *para-* substitutions with electron-withdrawing cyano and electron-donating methyl, and methoxy substituents at this subunit. Compounds 8 – 10 have the cyano substituent in the terminal phenylene of DSB derivatives without any substitution at the vinylene subunit. Table 2 shows the calculated absorption and emission spectra for these DSB derivatives. The *meta*-cyano DSB has the excitation energy of about 0.1eV (3.45 eV *vs.* 3.35 eV) higher than that of the *ortho-* and *para*-cyano DSB. Comparing the absorption λ_{max}, *meta*-cyano DSB exhibits the shorter wavelength at 359 *nm*, while *para-* and *ortho*-cyano DSB have the longer wavelength of around 370 *nm*. Thus, *ortho-* and *para*-cyano DSB show a red shift relative to the *meta*-cyano DSB. This calculated result agrees well with the experimental data. In particular, *ortho-* and *para-* substitutions result in the same excitation energy and absorption λ_{max}, so that they may have similar physical properties. To investigate the effect of various substituents in the terminal phenylene of DSB, we calculated the derivatives with the electron-donating methoxy and methyl substituents in *ortho-, meta-* and *para-* substitutions (Compounds 11 - 16). We obtained the following order of excitation

energies for DSB derivatives: *meta-* > *ortho-* > *para-*. This result is similar to that for cyano substituted DSB derivatives (Table 2). According to the semiempirical ZINDO/AM1 calculation, the *meta*-DSB derivative exhibits a blue shift in the electron transition spectra for the absorption and emission parameters as compared to the *para-* and *ortho*-DSB derivatives, respectively. Thus, the calculation indicate that the electron-donating and -withdrawing substituents do not influence the order of the excitation energy, absorption λ_{max} and emission λ_{max} in DSB derivatives. This conclusion also show that *para-* and *ortho-* substituents have the stabilization effect with respect to the π-electron delocalization in the π-system of DSB.

Compounds 17 – 22 are the methoxy and cyano substituents at the terminal phenylene with β-cyano group in the vinylene of the DSB moiety. The calculated results show that the excitation energy for *meta-* is around 0.02 eV ~ 0.07 eV higher than that for *ortho-* and *para-* substitutions. Thus, *ortho-* and *para-* substituents resulted in a red shift as compared to the *meta*-substituent in the terminal phenylene of DSB derivatives. The methoxy substituted DSB derivatives are also calculated to have the same transition parameters as those for cyano-substituted DSB. Since β-cyano group in the vinylene double band interact with the methoxy substituent in the terminal phenylene, it causes a distortion of the main backbone and increases the dihedral angle between the vinylene and the terminal phenylene of DSB. A comparison of the calculated absorption parameters of for compounds 8-10 and compounds 17-19 shows that the DSB derivatives with β-cyano substituent have lower excitation energy and exhibit the red shift in the spectra.

In order to calibrate the calculated results with experimental data, the plots of experimental vs. calculated absorption and emission spectra are shown in Figs. 2a and 2b. The corresponding regression equation are given as follows:

$\lambda_{exp} = 1.44\ \lambda_{calc} - 130.93$, $r^2 = 0{,}9201$. (Absorption spectrum),

$\lambda_{exp} = 1.17\ \lambda_{calc} - 10.28$, $r^2 = 0.9031$. (Emission spectrum).

The mean errors are 20 *nm* and 60 *nm* for the absorption and emission spectra, respectively.

Conclusions

The experiments have demonstrated that the DSB derivatives, which are oligomeric analogs of the PPV polymer, could be applied as dopants in the multi-layer OLED fabrication. The substitution effect on the central and terminal phenylene as well as vinylene subunit of DSB can vary the absorption and emission wavelength. The substitutions generate a red shift for *ortho-* and *para-* substituents as compared to the corresponding *meta*-substituent both for electron-donating and –withdrawing substituents in the terminal phenylene of DSB moiety. The α-substituent generated a blue shift relative to the β-substituent in the vinylene subunit of the DSB moiety. Actually, the related experimental works also confirmed the above computational results. This calculation procedure can be used as a model system for understanding the relationship between luminescence and molecular structure and also can be employed to explore the potential EL device and their applications.

Acknowledgement

We thank Dr. Alexander Mebel for reading the manuscript and the National Science Council of ROC for financially supporting this work.

References

1. P. de Silva, H. Q. N. Gunaratne, T. Gunnlaugsson, A. J. M. Huxley, C. P. McCoy, J. T. Rademacher, T. E. Rice, Chem. Rev. 97, 1515(1997).
2. C. E. Kerr, C. D. Mitchell, J. Headrick, B. E. Eaton, T. L. Netzel, J. Phys. Chem. B 104, 1637 (2000).
3. U. Stalmach, H. Detert, H. Meier, V. Gebhardt, D. Haarer, A. Bacher, H.-W. Schmidt, Opti. Mater., 9, 77 (1998).
4. K. Müllen, G. Wegner, Electronic Materials: The Oligomer Approach, Wiley-VCH (1998).
5. M. Leuze, M. Hohloch, M. Hanack, Chem. Mater., 14, 3339 (2002).
6. R. H. Young, C. W. Tang, A. P. Marchetti, Appl. Phys. Lett., 80, 874 (2002).
7. H. H. Hörhold, J. Opfermann, Makr. Chem., 131, 105 (1970).
8. C. W. Tang , S. A. Vanslyke, Appl. Phys. Lett., 51, 913 (1987)
9. N. C. Greenham, S. C. Moratti, D. D. C. Bradley, R. H. Friend, A. B. Holmes, Nature, 365, 628 (1993).
10. H. E. Katz, S. F. Bent, W. L. Wilson, M. L. Schilling, S. B. Ungashe, J. Am. Chem. Soc., 116, 6631 (1994).
11. L. M. Burroughs, D. D. C. Bradley, A. R. Brown, R. M. Marks, K. Mackey, R. H. Friend, P. L. Burns, A. B. Holmes, Nature, 347, 539 (1990).

12. F. –T. Luo, Y. –T. Tao, S. –L. Ko, C. –H. Chuen and H. Chen, J. Mater. Chem., 12, 47 (2002).
13. Y. Ichino, J. P. Ni, Y. Ueda, D. K. Wang, Synt. Meta., 116, 223 (2001).
14. R. Chang, J. H. Hsu, W. S. Fann, K. K. Liang, C. H. Chang, M. Hayashi, J. Yu, S. H. Lin, E. C. Chang, K. R. Chuang, S. A. Chen, Chem. Phys. Lett., 317, 142 (2000).
15. J. Yu, W. S. Fann, S. H. Lin, Theor. Chem. Acc., 103, 374 (2000).
16. W. M. F. Fabian, K. S. Niederreiter, G. Uray, W. Stadlbauer, J. Mole. Stru., 477, 209 (1999).
17. W. M. F. Fabian, J. M. Kauffman, J. Luminescence, 85, 137 (1999).
18. a. M. J. Frisch, G. W. Trucks, H. B. Schlegel, G. E. Scuseria, M. A. Robb, J. R. Cheeseman, V. G. Zakrzewski, J. A. Montgomery, R. E. Stratmann, J. C. Burant, S. Dapprich, J. M. Millam, A. D. Daniels, K. N. Kudin, M. C Strain, O. Farkas, J. Tomasi, V. Barone, M. Cossi, R. Cammi, B. Mennucci, C. Pomelli, C. Adamo, S. Clifford, J. Ochterski, G. A. Petersson, P. Y. Ayala, Q. Cui, K. Morokuma, D. K. Malick, A. D. Rabuck, K. Raghavachari, J. B. Foresman, J. Cioslowski, J. V. Ortiz, B. B. Stefanov, G. Liu, A. Liashenko, P. Piskorz, I. Komaromi, R. Gomperts, R. L. Martin, D. J. Fox, T. Keith, M. A. Al-Laham, C. Y. Peng, A. Nanayakkara, C. Gonzalez, M. Challacombe, P. M. W. Gill, B. G. Johnson, W. Chen, M. W. Wong, J. L. Andres, M. Head-Gordon, E. S. Replogle, J. A. Pople, Gaussian 98, Gaussian, Inc., Pittsburgh, 1998.
19. J. J. P. Stewart, Fujutsu Limited, Tokyo, Japan (2000).

Figure captions:

Figure 1 Structures of DSB and its derivatives

Figure 2a Plot of calculated *vs.* experimental absorption λ_{max}.

Figure 2b Plot of calculated *vs.* experimental fluorescence λ_{max}.

Fig.1

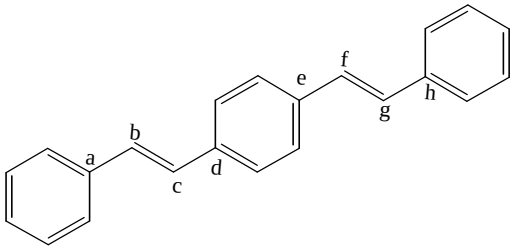

1: DSB

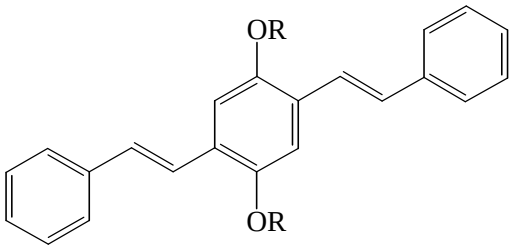

2: R = CH_3, 3: R = C_2H_5
4: R = C_3H_8, 5 R = C_6H_{13}

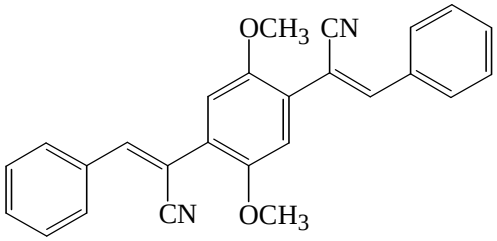

6

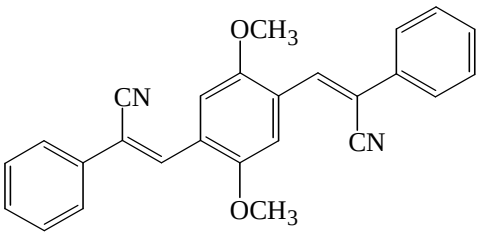

7

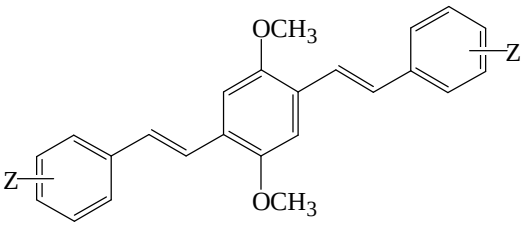

8: *Z* = *ortho*-CN,
9: *Z* = *meta*-CN,
10: *Z* = *para*-CN,
11: *Z* = *ortho*-OCH_3,
12: *Z* = *meta*-OCH_3,
13: *Z* = *para*-OCH_3,
14: *Z* = *ortho*-CH_3,
15: *Z* = *meta*-CH_3,
16: *Z* = *para*-CH_3.

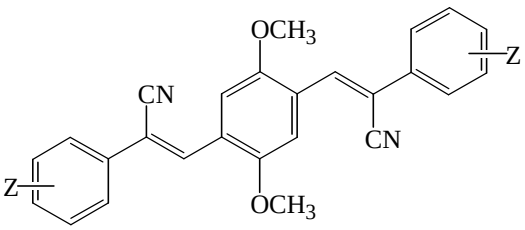

17: *Z* = *ortho*-CN,
18: *Z* = *meta*-CN,
19: *Z* = *para*-CN,
20: *Z* = *ortho*-OCH_3,
21: *Z* = *meta*-OCH_3,
22: *Z* = *para*-OCH_3.

Fig. 2a

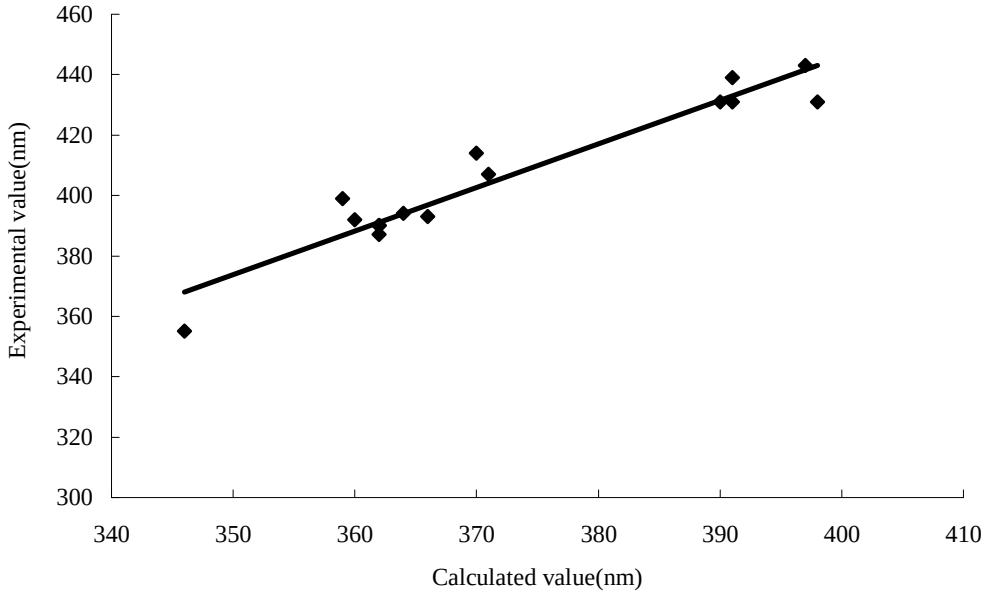
460
440
420
400
380
360
340
320
300
Experimental value(nm)
340
350
360
370
380
390
400
410
Calculated value(nm)

Fig. 2b

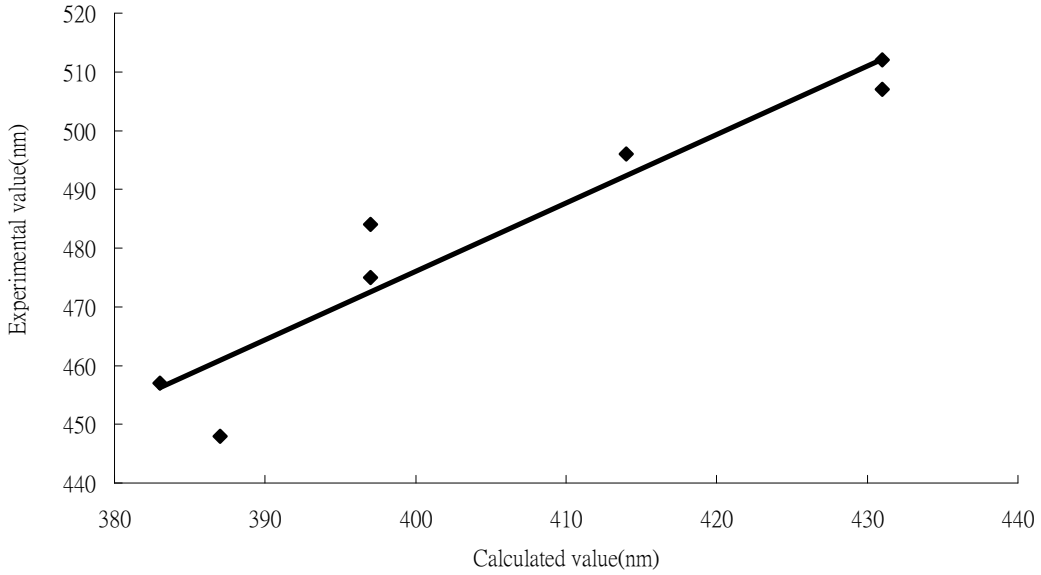

Table1 Calculated bond lengths (Å) of optimized DSB.*

	ab	bc	cd	ef	fg	gh
HF/6-31G	1.474	1.333	1.471	1.471	1.333	1.474
B3YLP/6-31G	1.467	1.354	1.463	1.463	1.354	1.467
AM1	1.452	1.344	1.452	1.452	1.344	1.452
PM3	1.457	1.342	1.456	1.456	1.343	1.457

*The structure of DSB is described in Fig. 1.

Table 2 Calculated HOMO (eV), LUMO (eV), ΔE (= LUMO - HOMO) (eV), absorption λ_{max} (*nm*), oscillator strength (*f*), excitation energy (eV), fluorescence λ_{max} (*nm*) as well as experimental absorption λ_{max} (*nm*) and fluorescence λ_{max} (*nm*) of DSB and its derivatives.

Cpd[a]	Calculated value							Experimental value[b]	
	HOMO	LUMO	ΔE	UV λ_{max}	*f*	excitation energy	fluorescence λ_{max}	UV λ_{max}	fluorescence λ_{max}
1	-8.19	-0.81	7.38	346	2.116	3.58	378	355	---
2	-7.96	-0.82	7.14	362	1.735	3.43	388	390*	---
3	-7.92	-0.79	7.13	362	1.734	3.42	388	390*	---
4	-7.92	-0.79	7.13	362	1.729	3.42	387	387	448
5	-7.92	-0.79	7.13	362	1.729	3.42	389	390	---
6	-8.33	-1.33	7.00	369	1.724	3.36	398	302*	---
7	-8.38	-1.49	6.89	391	1.662	3.17	418	431*	---
8	-8.18	-1.13	7.05	371	1.702	3.34	397	407*	475
9	-8.26	-1.11	7.15	359	1.786	3.45	383	399*	457
10	-8.03	-1.28	6.75	370	2.134	3.35	397	414*	484
11	-7.69	-0.62	7.07	366	1.788	3.38	394	393*	---

12	-8.01	-0.86	7.15	360	1.724	3.44	383	392*	---
13	-7.78	-0.69	7.09	364	1.919	3.40	391	394*	---
14	-7.91	-0.76	7.15	361	1.722	3.43	386	---	---
15	-7.90	-0.72	7.18	358	1.765	3.46	387	---	---
16	-7.87	-0.76	7.11	364	1.809	3.41	392	---	---
17	-8.51	-1.71	6.80	400	1.662	3.10	427	---	---
18	-8.67	-1.79	6.88	391	1.601	3.17	417	439*	---
19	-8.73	-1.92	6.81	397	1.870	3.12	426	443*	---
20	-8.11	-1.25	6.86	392	1.653	3.16	422	414*	496
21	-8.43	-1.57	6.86	390	1.683	3.18	418	431*	512
22	-8.21	-1.43	6.78	398	1.770	3.11	429	431*	507

[a]Compounds are denoted in Fig. 1.

[b]Ref. 12.

*There have hexyloxy substituent in the central phenylene of a DSB moiety.